Talbot holographic illumination nonscanning (THIN) fluorescence microscopy

Citation: Luo, Yuan, et al. "Talbot Holographic Illumination Nonscanning (THIN) Fluorescence Microscopy: Talbot Holographic Illumination Nonscanning (THIN) Fluorescence Microscopy." Laser & Photonics Reviews, vol. 8, no. 5, Sept. 2014, pp. L71–75.

As Published: http://dx.doi.org/10.1002/LPOR.201400053

Publisher: Wiley

Persistent URL: http://hdl.handle.net/1721.1/118927

Version: Author's final manuscript: final author's manuscript post peer review, without publisher's formatting or copy editing

Published in final edited form as:
Laser Photon Rev. 2014 September ; 8(5): L71–L75. doi:10.1002/lpor.201400053.

Talbot holographic illumination nonscanning (THIN) fluorescence microscopy

Yuan Luo[#1,2,*], **Vijay Raj Singh**[#3,*], **Dipanjan Bhattacharya**[#3,4,5], **Elijah Y. S. Yew**[#3,6], **Jui-Chang Tsai**[1], **Sung-Liang Yu**[7], **Hsi-Hsun Chen**[1,2], **Jau-Min Wong**[8], **Paul Matsudaira**[3,4,5], **Peter T. C. So**[3,6,9], and **George Barbastathis**[3,6]

[1]Center for Optoelectronic Biomedicine, College of Medicine, National Taiwan University, Taipei, 10051, Taiwan R.O.C

[2]Molecular Imaging Center, National Taiwan University, Taipei, 10055, Taiwan R.O.C

[3]Singapore-MIT Alliance for Research and Technology (SMART) Centre, 1 CREATE Way, #10-01 CREATE Tower, 138602, Singapore

[4]Centre for BioImaging Science (CBIS), Blk S1A, Level 2, National University of Singapore, 14 Science Drive 4, 117546, Singapore

[5]MechanoBiology Institute (MBI), National University of Singapore, 117411, Singapore

[6]Department of Mechanical Engineering, Massachusetts Institute of Technology, Cambridge, Massachusetts, 02139, USA

[7]Department of Clinical Laboratory Sciences and Medical Biotechnology, College of Medicine, National Taiwan University, Taipei, 10055, Taiwan R.O.C

[8]Department of Internal Medicine, National Taiwan University Hospital, Taipei, 10048, Taiwan, R.O.C

[9]Department of Biomedical Engineering, Massachusetts Institute of Technology, Cambridge, Massachusetts, 02139, USA

[#] These authors contributed equally to this work.

Abstract

Optical sectioning techniques offer the ability to acquire three-dimensional information from various organ tissues by discriminating between the desired in-focus and out-of-focus (background) signals. Alternative techniques to confocal, such as active structured illumination, exist for fast optically sectioned images, but they require individual axial planes to be imaged consecutively. In this article, an imaging technique (THIN), by utilizing active Talbot illumination in 3D and multiplexed holographic Bragg filters for depth discrimination, is demonstrated for imaging in vivo 3D biopsy without mechanical or optical axial scanning.

[*]Corresponding authors: yuan_luo@ntu.edu.tw; vrsingh@smart.mit.edu.

Supporting Information: for this article is available free of charge under http://dx.doi.org/10.1002/lpor.201400053

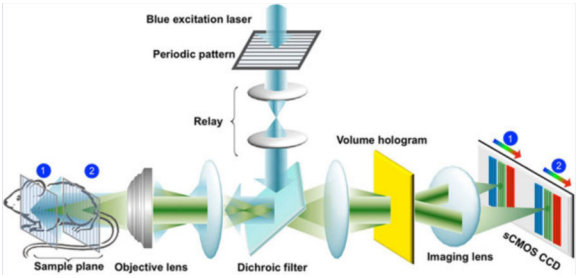

Keywords

3D wide field Microscopy; optical sectioning; holographic Bragg filters; Talbot effect

Wide-field fluorescence microscopy is a commonly used imaging technique by researchers and clinicians. A standard wide-field microscope has no optical sectioning capabilities and this limits its use in imaging thick biological samples. Although standard wide-field fluorescence microscopy with deconvolution techniques can improve image quality [1], it does not provide true optical sectioning, due to the missing cone in the system's transfer function. The most commonly used optical sectioning imaging method with good background rejection in biomedicine is based on the confocal approach [2–4]. However, the price to pay for improved image quality in 3D confocal microscopy is a point-by-point scan time that is proportional to the number of desired voxels, (i.e. the 3D space–bandwidth product) and high photobleaching. There exists a wealth of alternatives to confocal microscopy, most of which involve some form of active illumination to improve contrast and thus effectively reduce scanning time and improve image quality. Some recent examples are structured illumination microscopy (SIM) [5, 6], optical holographic microscopy (OHM) [7–12], digital scanned light-sheet microscopy (DSLM), its close relative selective plane illumination microscopy (SPIM) [13, 14], and HiLo imaging [15–17]. SIM overcomes the missing-cone problem, and speeds up the 3D image formation process through the use of wide-field excitation by structured illumination and the use of computational reconstruction algorithms where the illumination structure is exploited to improve the condition of the inverse problem. Although it is faster than confocal microscopy, SIM still requires the excitation plane to be scanned to construct a 3D image. OHM replaces scanning with deconvolving the image with the coherent Fresnel propagation kernel at multiple depths along the sample. Unfortunately, coherent propagation does not yield true 3D images except in the limit of a sparsely populated volume and thus it is not applicable for thick-tissue imaging [18]. To have any hope of recovering 3D structure information from denser samples such as tissue, the emission must be incoherent; indeed, fluorescence imaging is the most commonly used modality in 3D microscopy. Optical scanning holography [10] decoheres the image formation process for that reason, but it is still a technique based on point-by-point scanning and low numerical aperture (NA). More recently, methods based on a wavelength-encoding strategy and specially designed thin blazed gratings have been used for fast 3D imaging [19, 20]. However, both approaches still require mechanical scanning along at least one axis.

A radically different approach to 3D imaging with high speed and high contrast has been based on the related DSLM and SPIM approaches. In both cases excitation/illumination and detection are done crosswise so that the camera is positioned to capture the image of the entire illuminated plane at once. DSLM improves over SPIM by scanning a pencil-like beam faster than the camera frame rate to effectively provide a plane of illumination. Both techniques enable optical sectioning and the sample is exposed to less radiation, so they are suited to imaging live biological processes over a prolonged period. However, because the illuminated volume is larger than a focused spot, the background is necessarily also stronger than in the confocal case. A contrast-improvement mechanism is, therefore, needed and may be sought among two recently proposed approaches: Three-phase [15] and HiLo [17] illumination. Both techniques essentially amount to different strategies of spatial phase locking onto a sinusoidal actively illuminated pattern projected on the sample, but are geared toward imaging a single plane. A combination of modulated DSLM with HiLo reconstruction that we call “3D HiLo” can be used to remove background scattering and yield improved contrast through an entire volume albeit still at the cost of scanning [21].

In this paper, we demonstrate, to the best of our knowledge, the first experimental realization of a high-resolution, nonscanning, wide-field optically sectioned microscope for 3D imaging of tissue where contrast and speed are achieved from a combination of an active 3D sinusoidal illumination based on the Talbot effect and multiplexed holographic Bragg imaging filters (MHBFs) for space-variant image formation in fluorescence imaging. The Talbot holographic illumination nonscanning (THIN) system does not require any scanning for in vivo 3D biopsy of tissues, and allows the experimenter to define the condition of the inverse problem for computational reconstruction. The parallelism allowing the complete elimination of scanning is provided by the MHBFs, while the active Talbot sinusoidal illumination provides depth contrast and suppression of scattered light. It is important to emphasize that, as in Refs. [22–24], the use of a hologram is limited to a fixed, prerecorded element placed in the optical train that needs to be fabricated only once for each system. This is an important difference compared to the aforementioned holographic alternatives [11,12]. Since THIN does not require the formation of a hologram during imaging, it is compatible with fluorescence-based methods of imaging.

The THIN principle is based on acquiring pair-wise multidepth resolved images, one with Talbot-effect grid-pattern illumination, and the other with standard uniform illumination. A schematic diagram of the THIN microscope is shown in Fig. 1 for epifluorescence imaging. A grid of period d placed in the illumination path and illuminated using a coherent or partially coherent light source at central wavelength λ will form multiple images spaced by regular intervals at $2nd^2/\lambda$ along the optical axis z according to the Talbot effect [25]. The geometry is configured such that several of these Talbot planes occur inside the specimen (of refractive index n) and also serve as the input focal planes for the subsequent multiplex holographic Bragg filter (MHBF) [22,23].

The MHBF is formed by multiple exposures of a thick holographic material, each time exposing the material to the interference pattern of a spherical and a plane wave (hologram multiplexing). The angle of incidence of the plane wave increases in each exposure to change the corresponding multiplexed hologram’s spatial carrier. The origin of the spherical

waves also moves along the optical axis correspondingly at each exposure to match the distances of the Talbot planes to the system's entrance pupil. The MHBF so recorded behaves as a spatial-spectral filter. In this work, the spatial depth filtering property is used to simultaneously image two or more Talbot-defined depths onto different nonoverlapping lateral locations at the collective lens' image plane (i.e. CCD location) while the spectral filter determines the field of view for each imaged depth [22]. Specific layer separation and arbitrary arrangement of the projection angle are designed during the MHBF recording process. It is worth emphasizing that this Talbot-inspired illumination can be thought of as nonuniform illumination in both the transverse and axial directions leading to optically sectioned imaging at multiple depths without the need for axial scanning. In that sense, it is a 3D generalization of the HiLo principle. More information about the design of MHBFs and algorithm of Talbot-inspired illumination to simultaneously remove out-of-focus light in multiple depths and the MHBF design principle as well as recording process can be found in the Supplemental Materials section.

The ability of a THIN microscope to resolve volumetric samples was verified by imaging fluorescence labeled beads (25 μm diameter, Polysciences) suspended in a 1-mm thick slab of agarose (Invitrogen). The beads were excited using a blue tunable laser source (Innova 304C, Coherent Inc.) at λ = 488 nm. A dichroic mirror (Q505lp, Chroma Technology Corp.) was utilized, and an emission filter (MF530/43, Thorlabs Inc.) rejected stray excitation light during imaging. Figure 2 provides comparisons of standard 3D wide-field and optical sectioning images captured using THIN. Two depth-resolved images with out-of-focus light at both planes are simultaneously captured from the CCD with uniform illumination and are shown in Fig. 2a; the depth separation between two planes is 45 μm, and can be controlled by tuning the separation distance during exposures (as shown in supplementary material) [23], or adjusting emission wavelength [24]. The THIN system had an effective magnification of 5.6× using an Olympus objective lens (ULWDMSPlan50X, NA0.55). The MHBF consisted of two multiplexed gratings with diffraction efficiencies of ~35% and 40% capable of simultaneously imaging planes with 45 μm depth separation. The imaging lens was a Mitutoyo objective (MPlanAPO20X, NA0.42), and the camera was Hamamatsu ORCA4.0 sCMOS. Figure 2c shows the resultant THIN images, processed by using the uniform illuminated images (Fig. 2a) and Talbot-inspired structured illuminated images with 170 lines-per-millimeter (lpm) (Fig. 2b). The HiLo principle for THIN was used to remove the out-of-focus background noise from the desired in-focus signal. As a comparison, the same region of the sample was imaged using a Zeiss confocal scanning microscope (LSM510, Carl Zeiss Germany) with a Zeiss 10× NA 0.3 objective (EC Plan-Neofluar10X). The captured images, corresponding to the same axial planes, from conventional laser scanning confocal microscopy are shown in Fig. 2d. Figure 2e compares local contrast and out-of-focus background rejection, by plotting an intensity profile along a line, between the different techniques. The system's depth resolution is quantified experimentally by plotting the grid contrast along the axial direction. For a projected grid of spatial frequency 120 lpm, the depth resolution of the system is 25 μm. (More information about THIN methodology, resolution in both lateral and axial directions, contrast plots of the imaging grid as function of axial direction and quantitative comparison of imaging performance of THIN microscopy with different imaging modalities for fluorescence beads can be found in the Supplemental

Materials section.) It is worth mentioning that with grids of higher frequencies the system can simultaneously provide finer optical sectioning [26] at multiple depths without scanning.

The experiment with beads is a situation where the sample is sparse. In reality, practical imaging often involves samples that are highly scattering. We used mice intestine to test the performance of the THIN microscope under more difficult in vivo conditions.

To demonstrate the in vivo imaging capability of the microscope, we performed an experiment to image the intestine of a live mouse on THIN microscope. We kept an anesthetized mouse on a specially designed imaging chamber (as shown in the Supplementary Material) [27] and mounted the mouse on THIN microscope, before performing in vivo imaging experiment. Figure 3 shows the in vivo images of villi of mouse intestine sample as taken with our THIN microscope. As in the case of the beads, two planes, separated by 45 μm, were imaged simultaneously onto different parts of the camera. Figure 3a was taken with uniform illumination, i.e. without the Talbot grating. The MHBF still succeeds at imaging the two planes, separated by 45 μm, to adjacent regions of the camera. However, haze is significantly visible due to the thick nature of the sample and the wide-field illumination. Figure 3b shows the effective removal of the haze when we utilized the complete THIN principle, including Talbot-structured illumination and HiLo postprocessing. The background has been suppressed significantly and low-contrast features are now clearly visible. Figures 3c–e show the time-lapse resultant images at depths 1 and 2 of the dashed boxed highlighted in Fig. 3b, and time-lapse animation of imaging in vivo mouse intestine can be found in the Supplemental Material. Changes on the villi structures over a period of 900 s can be clearly observed. Figure 3f shows intensity cross sections comparing the signal-to-background with uniform illumination and THIN illumination at depths 1 and 2. (Additional information on the experimental procedure, comparison to confocal scanning, and results of an in vitro mice intestine experiment can be found in the Supplementary Material.)

In conclusion, we have developed, for the first time to our knowledge, a nonscanning, wide-field optical sectioning microscope to simultaneously observe in vivo 3D images from different planes within a volumetric tissue sample while effectively rejecting out-of-focus background. The THIN system is simple, robust, and cost-effective; it also promises to increase throughput significantly as it captures multiple planes simultaneously. This is advantageous when imaging time-sensitive processes occurring in different planes. The system can be extended to obtain more planes simultaneously with more MHBFs within a volume hologram using PQ-PMMA or other recording materials [28–32]. Although the grating is inserted manually with the current system, it is possible to use a spatial light modulator to switch between structured and uniform illumination. It is also possible to reconstruct the entire image with a faster computing device in a fully automated fashion with more MHBFs, ultimately enabling real-time 3D video microscopy.

Supplementary Material

Refer to Web version on PubMed Central for supplementary material.

Acknowledgements

We acknowledge financial support from the U.S. National Institutes of Health (NIH RO1CA134424), the National Research Foundation, Singapore through the Singapore MIT Alliance for Research and Technology's BioSystems and Micromechanics Inter-Disciplinary Research programme (015824-039), the Taiwan National Science Council (100-2218-E-002-026-MY3, 102-2218-E-002-013-MY3), National Taiwan University (103R7832), National Taiwan University Hospital (UN103-028), and Taiwan National Health Research Institutes (EX103-10220EC). P. So further acknowledges support from NSF funding for EBICS (CBET-0939511) and NIH funding for LBRC (9P41EB015871-26A1). We thank Chih-Ju Lin and Hans Hu for sample preparations and Confocal image analysis, and also thank Chen Yuan Dong for valuable comments.

References

[1]. McNally JG, Karpova T, Cooper J, Conchello JA. Methods. 1999; 19:373–385. [PubMed: 10579932]

[2]. Minsky, M. US patent 3013467. 1961.

[3]. Sheppard CJR, Choudhury A. Optica Acta. 1977; 24:1051–1073.

[4]. Conchello J-A, Lichtman JW. Nature Methods. 2005; 2:920–931. [PubMed: 16299477]

[5]. Neil M, Juskaitis R, Wilson T. Opt. Lett. 1997; 22:1905–1907. [PubMed: 18188403]

[6]. Kner P, Chhun BB, Griffis ER, Winoto L, Gustafsson MGL. Nature Methods. 2009; 6:339–342. [PubMed: 19404253]

[7]. Gabor D. Nature. 1948; 161:777–778. [PubMed: 18860291]

[8]. Garcia-Sucerquia J, Xu W, Jericho SK, Klages P, Jericho MH, Kreuzer HJ. Appl. Opt. 2006; 45:836–850. [PubMed: 16512525]

[9]. Leith EN, Chien W-C, Mills KD, Athey BD, Dilworth DS. J. Opt. Soc. Am. A. 2003; 20:380–387.

[10]. Poon T-C. J. Opt. Soc. Am. A. 1985; 2:521–527.

[11]. Rosen J, Brooker G. Opt. Exp. 2007; 15:2244–2250.

[12]. Rosen J, Brooker G. Nature Photon. 2008; 2:190–195.

[13]. Keller PJ, Schmidt AD, Wittbrodt J, Stelzer EHK. Science. 2008; 322:1065–1069. [PubMed: 18845710]

[14]. Keller PJ, Schmidt AD, Santella A, Khairy K, Bao Z, Wittbrodt J, Stelzer EHK. Nature Methods. 2010; 7:637–642. [PubMed: 20601950]

[15]. Karadaglic D, Wilson T. Micron. 2008; 39:808–818. [PubMed: 18337108]

[16]. Santos S, Chu KK, Lim D, Bozinovic N, Ford TN, Hourtoule C, Bartoo AC, Singh SK, Mertz J. J. Biomed. Opt. 2009; 14:030502. [PubMed: 19566286]

[17]. Mertz J. Nature Methods. 2011; 8:811–819. [PubMed: 21959136]

[18]. Tian L, Loomis N, Dominguez-Caballero JA, Barbastathis G. Appl. Opt. 2010; 49:1549–1554. [PubMed: 20300149]

[19]. Abrahamsson S, Chen J, Hajj B, Stallinga S, Katsov AY, Wisniewski J, Mizuguchi G, Soule P, Mueller F, Darzacq CD, Darzacq X, Wu C, Bargmann CI, Agard DA, Dahan M, Gustafsson MGL. Nature Methods. 2013; 10:60–63. [PubMed: 23223154]

[20]. Yelin D, Rizvi I, White WM, Motz JK, Hasan T, Bouma BE, Tearney GJ. Nature. 2006; 443:765. [PubMed: 17051200]

[21]. Bhattacharya D, Singh VR, Zhi C, So PTC, Matsudaira P, Barbastathis G. Opt. Exp. 2012; 20:27337–27347.

[22]. Liu W, Psaltis D, Barbastathis G. Opt. Lett. 2002; 27:854–856. [PubMed: 18007950]

[23]. Luo Y, Oh S, Barbastathis G. Opt. Lett. 2010; 35:781–783. [PubMed: 20195351]

[24]. Barbastathis, G.; Psaltis, D. Volume holographic multiplexing methods. In: Coufal, HJ.; Psaltis, D.; Sincerbox, GT., editors. Holographic Data Storage, Springer Series in Optical Sciences. 1st edn. Vol. 76. Springer; Berlin: 2000. p. xxvi

[25]. Goodman, J. Introduction to Fourier Optics. 3rd edn. Roberts and Company; Englewood, CO: 2005.

[26]. Choi H, Yew EYS, Hallacoglu B, Fantini S, Sheppard CJR, So PT, Biomedical C. Opt. Exp. 2013; 4:995–1005.

[27]. Liu Y, Chen HC, Yang SM, Sun TL, Lo W, Chiou LL, Huang GT, Dong CY, Lee HS. J. Biomed. Opt. 2007; 12:014014–014014-5. [PubMed: 17343489]

[28]. Luo Y, Gelsinger PJ, Barton JK, Barbastathis G, Kostuk RK. Opt. Lett. 2008; 33:566–568. [PubMed: 18347711]

[29]. Gerke TD, Piestun R. Nature Photon. 2010; 4:188–193.

[30]. Luo Y, Russo JM, Kostuk RK, Barbastathis G. Opt. Lett. 2010; 35:1269–1271. [PubMed: 20410989]

[31]. Moser C, Maravic I, Schupp B, Adibi A, Psaltis D. Opt. Lett. 2000; 25:1243–1245. [PubMed: 18066180]

[32]. Blanche Q-A, Bablumian R, Voorakaranam R, Christenson C, Lin W, Gu T, Flores D, Wang P, Hsieh W-Y, Kathaperumal M, Rachwal B, Siddiqui O, Thomas J, Norwood RA, Yamamoto M, Peyghambarian N. Nature. 2010; 468:80–83. [PubMed: 21048763]

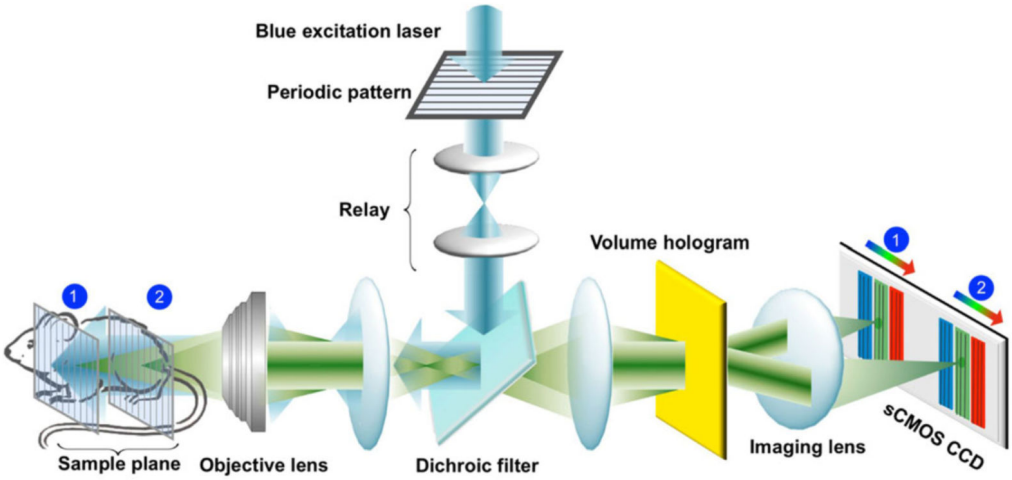

Figure 1.

Schematic drawing of the THIN microscope in epifluorescence format. In this diagram, signal from the sample emanates from two axially separated planes (1 and 2). The axial separation between the two planes is converted to a shift in the transverse direction by the combination of volume hologram and imaging lens, and is recorded as two images side-by-side on the detector. This transverse separation is accomplished using an MHBF (see text) positioned at the Fourier plane. For each plane, the MHBF diffracts the fluorescence emission at different angles based on the wavelength. Imaged planes are separated at some lateral separation specified by the focal length of the collection lens. The system was illuminated with a periodic grid pattern to induce the Talbot effect onto the object plane at multiple depths (see text).

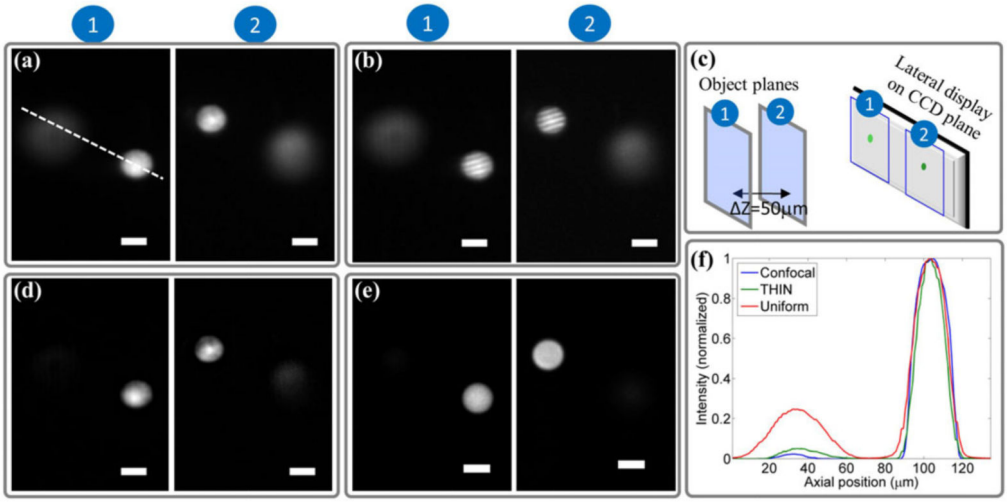

Figure 2.

(a) Uniform illuminated, and (b) Structured illuminated images of 25-μm fluorescence beads for the two axial planes. (c) Imaging scheme of the THIN system. (d) THIN images at the corresponding axial planes, obtained using pair-wise imaging algorithm that requires respective column of (a) and (b). (e) Confocal (Zeiss LSM 510) scanning microscopic images of the same observable axial planes. Scale bar indicates 20 μm size. (f) Intensity profile at the signal (focus beads) and background (defocus beads).

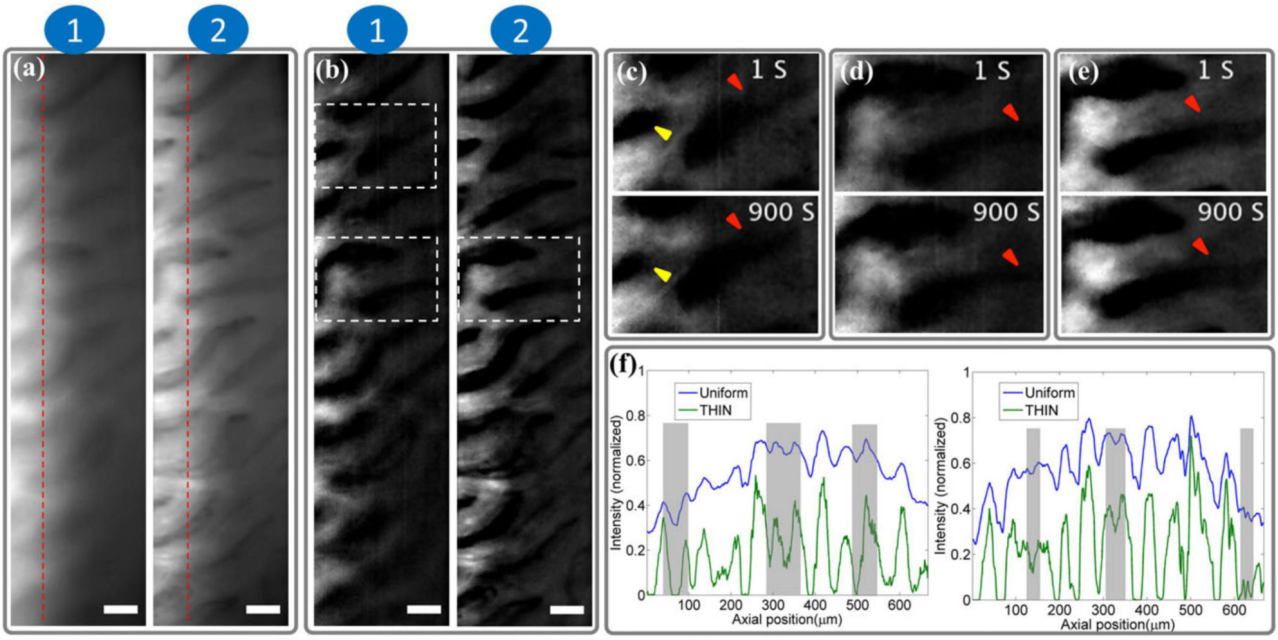

Figure 3.

(a) In vivo uniformly illuminated images of fluorescently labeled mice intestine sample obtained from two axially separated planes (1 and 2), respectively using the same imaging system of Fig. 2. Mouse intestine was stained with Rhodamine 6G (Sigma, Saint Louis, Missouri). (b) Corresponding THIN images using the proposed THIN algorithm. Scale bars are 20 μm in length. (c)–(e), Zoom-in to the dashed-box region of (b), respectively (showing the features at plane 1 and 2 in time-lapse mode). (f) Intensity cross section along the red lines shown in plane 1 and 2 of the uniformly illuminated and THIN-illuminated images (a) and (b), respectively.